Human Molecular Genetics, 2010, Vol. 19, No. 2 ***329–341***
doi:10.1093/hmg/ddp499
Advance Access published on November 9, 2009

Nesprin 1 is critical for nuclear positioning and anchorage

Jianlin Zhang[1], Amanda Felder[3], Yujie Liu[1], Ling T. Guo[2], Stephan Lange[1], Nancy D. Dalton[1], Yusu Gu[1], Kirk L. Peterson[1], Andrew P. Mizisin[2], G. Diane Shelton[2], Richard L. Lieber[3] and Ju Chen[1,*]

[1]Department of Medicine and [2]Department of Pathology, University of California San Diego, La Jolla, CA 92093, USA and [3]Department of Orthopaedic Surgery and Bioengineering, University of California San Diego and Veterans Affairs Medical Centers, San Diego, CA 92161, USA

Received August 25, 2009; Revised October 19, 2009; Accepted October 26, 2009

Nesprin 1 is an outer nuclear membrane protein that is thought to link the nucleus to the actin cytoskeleton. Recent data suggest that mutations in Nesprin 1 may also be involved in the pathogenesis of Emery-Dreifuss muscular dystrophy. To investigate the function of Nesprin 1 *in vivo*, we generated a mouse model in which all isoforms of Nesprin 1 containing the C-terminal spectrin-repeat region with or without KASH domain were ablated. Nesprin 1 knockout mice are marked by decreased survival rates, growth retardation and increased variability in body weight. Additionally, nuclear positioning and anchorage are dysfunctional in skeletal muscle from knockout mice. Physiological testing demonstrated no significant reduction in stress production in Nesprin 1-deficient skeletal muscle in either neonatal or adult mice, but a significantly lower exercise capacity in knockout mice. Nuclear deformation testing revealed ineffective strain transmission to nuclei in muscle fibers lacking Nesprin 1. Overall, our data show that Nesprin 1 is essential for normal positioning and anchorage of nuclei in skeletal muscle.

INTRODUCTION

Emery-Dreifuss muscular dystrophy (EDMD) is a form of muscular dystrophy characterized by progressive skeletal muscle weakness, with associated muscle contractures and variable cardiac defects (1). Forty percent of patients with EDMD have been shown to have mutations in either Emerin or Lamin A/C (LMNA), two genes encoding proteins localized to the inner nuclear membrane (INM) and its underlying lamina, respectively (2). The INM, outer nuclear membrane (ONM) and the nuclear lamina comprise the nuclear envelope, which is linked to the cytoskeleton by members of both the SUN and Nesprin protein families. Approximately 60% of EDMD patients do not have mutations in either Emerin or LMNA, suggesting that other genes are involved in EDMD (2). Recent data suggest that missense mutations in Nesprins 1 and 2 may also be involved in the pathogenesis of EDMD (3). Mutation of Nesprin 1 has also been found to be responsible for autosomal recessive arthrogryposis, another disease characterized by progressive muscle weakness (4).

Nesprins belong to a newly discovered family of mammalian spectrin-repeat (SR) proteins (5) that consists of four members, Nesprins 1–4 (6–8). Use of alternative promoters, polyadenylation sites and RNA splicing generate multiple isoforms of Nesprin 1 (also known as Syne1, myne1 and Enaptin) and Nesprin 2 (also known as Syne2 and NUANCE) that vary greatly in size (9). Giant (G) isoforms of Nesprin 1 and Nesprin 2 contain two N-terminal calponin-homology (CH) domains that bind actin filaments, an SR containing rod domain, and a C-terminal transmembrane KASH (Klarsicht/Anc/Syne homology) domain (10,11). Other isoforms of Nesprins 1 and 2 lack the N-terminal CH domains and/or the C-terminal KASH domain and also contain a much smaller SR rod domain (5). Nesprins 1 and 2 are anchored in the ONM through the interaction of their C-terminal KASH domains with the SUN (Sad1p/UNc-84) domains of

*To whom correspondence should be addressed at: Department of Medicine, University of California San Diego, 9500 Gilman Drive, BSB, Room 5025, La Jolla, CA 92093-0613, USA. Tel: +1 8588224276; Fax: +1 8585342069; Email: juchen@ucsd.edu

INM proteins SUN1 and SUN2 within the perinuclear space (12–14). In transgenic mice lacking both SUN proteins, Nesprin 1 fails to localize at the ONM (14). The SUN proteins bind to the nuclear lamins within the INM, forming a connection from the nuclear lamina to the cytoskeleton that has been termed the LINC complex (linker of nucleoskeleton and cytoskeleton) (12,15).

Previous studies of the Nesprins have suggested roles in nuclear envelope structure. One study revealed an increase in the perinuclear space between the ONM and INM in HeLa cells when Nesprin 2G was displaced by siRNA knockdown of SUN1 and SUN2. In addition to its interaction with the SUN proteins, smaller isoforms of Nesprin 1 have also been shown to interact with Lamin A/C *in vivo* and Emerin *in vitro*, further supporting its roles in stabilizing the nuclear lamina and regulating the nuclear intramembrane spacing (16,17). *In vitro* knockdown of Nesprin 1 alpha and beta isoforms in U20S and fibroblast cells leads to nuclear morphological defects similar to those seen in cells from EDMD patients. Additionally, Emerin and SUN2 are mislocalized in these transfected cells (3).

The giant isoforms of Nesprin, Nesprin 1G and Nesprin 2G are thought to provide a linkage between the nuclei and actin cytoskeleton, and thus could mediate its proposed role in nuclear localization. Previous studies in *Drosophila* and *Arabidopsis* demonstrated that nuclear positioning is dependent on actin polymerization, suggesting that the actin cytoskeleton anchors the nuclei (18,19). Mutation in the *Caenorhabditis elegans* ortholog of Nesprin 1G, anc-1, causes nuclear mislocalization within syncytial hypodermal cells (20,21). In addition, the N-terminal CH domains of Nesprin 1G have been shown to interact directly with actin, suggesting that this interaction may be responsible for nuclear anchorage (10). One study on mice in which a dominant-interfering Nesprin 1 transgene was overexpressed found that fewer synaptic nuclei were present in transfected muscle fibers (22).

Several groups have created lines of gene-targeted mice in which parts of the Nesprin protein have been removed or replaced in order to better understand its function. In one study, mice lacking the actin-binding domain of Nesprin 2G were found to be almost indistinguishable from wild-type mice, except for slight epidermal thickening (23). Fibroblasts from these mice exhibited abnormal nuclear morphology and uneven distribution of Emerin in the nuclear envelope. No defects were observed in skeletal muscle, and viability was not affected. In another study, selective ablation of the KASH domain of either Nesprin 1 (Nesprin $1^{\delta KASH}$) or Nesprin 2 (Nesprin $2^{\delta KASH}$) in mice did not affect either viability or fertility, but mutants missing the KASH domain of both of these proteins died within 20 min of birth from respiratory failure (24). Interestingly, the deletion of the KASH domain of Nesprin 1, but not of Nesprin 2, caused abnormal positioning of non-synaptic nuclei and disappearance of clusters of synaptic nuclei in skeletal muscle (24). Heart and muscle function of these mice was not investigated. A recent study of Nesprin 1 mutant mice (Nesprin 1^{rKASH}), in which the KASH domain was specifically replaced by a stretch of unrelated C-terminal amino acids, found that approximately half of the mutant homozygous mice died at birth from respiratory failure (25). Surviving mice exhibited cardiac conduction defects, kyphoscoliosis, small body mass and mislocation and clumping of muscle fiber nuclei, but had normal localization of Nesprin 1, Lamin A/C, Emerin and SUN2 at the nuclear envelope. Young adult female mice were less coordinated than their wild-type littermates, although tests of exercise capacity and muscle force generation were not performed.

To supply further insight into the functions of Nesprin 1, we generated a mouse model in which all isoforms of Nesprin 1 containing the C-terminal SR region with or without KASH domain (hereafter referred to as Nesprin $1^{-/-}$ mice). We show that Nesprin $1^{-/-}$ mice are marked by decreased survival rates, growth retardation and increased variability in body weight. We were able to further clarify Nesprin 1's roles in nuclear positioning and anchorage, nuclear membrane structure and cardiac mechanics, as well as investigate Nesprin 1's role in skeletal muscle function, exercise capacity and nuclear mechanics.

RESULTS

Generation of Nesprin 1 knockout mice

To study the *in vivo* function of Nesprin 1, we generated Nesprin 1-deficient mice by gene targeting. The two published Nesprin 1 mutant mice were generated either by partially removing (24) or completely replacing (25) the last Nesprin 1 exon which encodes the KASH domain. Since it has been shown that there are Nesprin 1 splicing isoforms without the KASH domain (26), and to ensure that all isoforms of Nesprin 1 containing C-terminal domains (5) would be ablated, a construct was designed to target a C-terminal exon that is shared by all Nesprin 1 isoforms containing the C-terminal SR region with or without KASH domain (Supplementary Material, Fig. S1A and S2). The targeted exon was the 16th exon as counted backward from the last exon. The 16th exon is the second coding exon of Nesprin-1α (also named syne 1A, myne-1), which is highly expressed in cardiac and skeletal muscle (17,27,28) (also see Supplementary Material, Fig. S2A). After electroporation of the targeting vector into R1 embryonic stem (ES) cells, two clones that had undergone homologous recombination were identified by Southern blot analysis (Supplementary Material, Fig. S1B). The clones gave rise to chimera mice that were then bred with Black Swiss mice to generate germ line-transmitted heterozygous Nesprin $1^{f/+}$ mice. These mice were subsequently mated with Protamine-Cre mice (29) to generate heterozygous Nesprin $1^{f/+,\ C/+}$ mice, which were then crossed with Black Swiss mice to generate Nesprin $1^{+/-}$ mice.

The heterozygotes were used as breeders to generate Nesprin $1^{-/-}$ mice and Nesprin $1^{+/+}$ littermates for experiments. To verify that homozygous knockout mice were null mutants, we performed RT–PCR analysis with mRNA samples from wild-type and mutant mice. RT–PCR of sequences between the 18th and 13th exons (as counted backward from the last exon) was performed. Whereas the expected 787 bp product was amplified from the WT sample, a product of 644 bp was detected in samples from Nesprin $1^{-/-}$ mice (Supplementary Material, Fig. S1E).

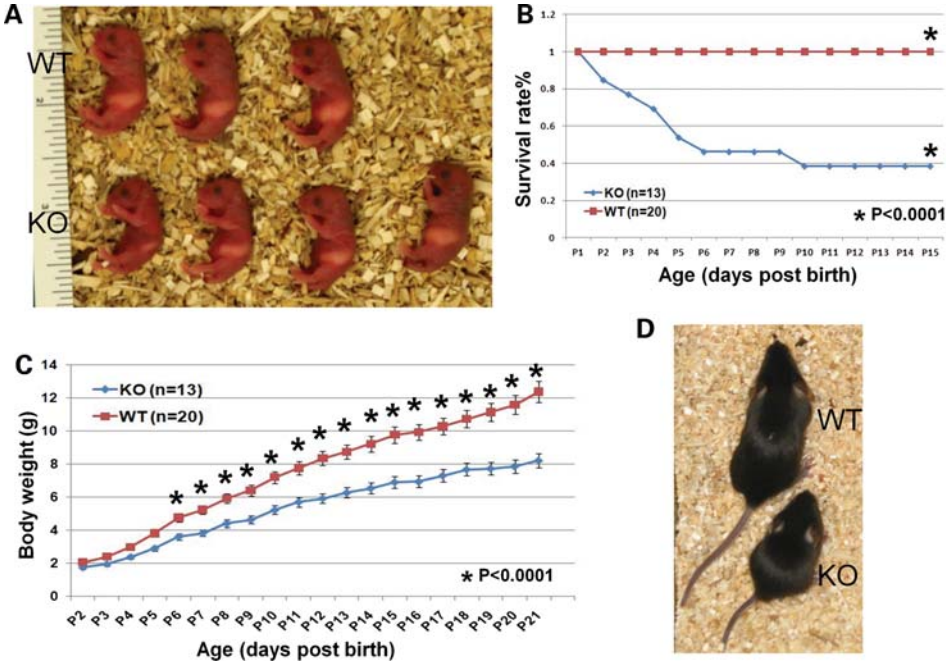

Figure 1. Absence of Nesprin 1 affects viability. (**A**) Nesprin 1 knockout mice at post-natal day 1 compared with wild-type littermate controls. Wild-type pups shown above, knockout pups below. (**B**) Typical survival curve of Nesprin 1 knockout mice. (**C**) Typical growth curve of Nesprin 1 knockout mice and wild-type littermates from birth until weaning. (**D**) Body size of Nesprin 1 knockout mouse compared with wild-type littermate at 21 days of age.

Sequence analysis of the aberrant PCR product revealed that it was identical to the wild-type product, except the 16th exon was missing (data not shown). Removal of the 16th exon led to a premature stop codon in the 13th exon (Supplementary Material, Fig. S2).

We then performed western blot and immunostaining analysis with a Nesprin 1 antibody generated against sequence 841-GRSTPNRQKSPRGKC-855 from Nesprin 1α (synaptic nuclear envelope 1 isoform 2, NP_071310.2) (also see Supplementary Material, Fig. S2B). Western blot results (Supplementary Material, Fig. S1D) clearly demonstrated that two protein bands, one at ∼120 kDa and one much larger than 200 kDa, are present in the wild-type samples, but are absent in the mutant samples. The 120 kDa band and the protein much larger than 200 kDa correspond to the molecular weights of Nesprin 1α (synaptic nuclear envelope 1 isoform 2, NP_071310.2) and the synaptic nuclear envelope 1 isoform 3 (NP_001073154.1), respectively. These are the only two mouse Nesprin 1 isoforms containing the C-terminal SR region and the KASH domain listed in NCBI website (http://www.ncbi.nlm.nih.gov/gene/64009?ordinalpos=6&itool=EntrezSystem2.PEntrez.Gene.Gene_ResultsPanel.Gene_RVDocSum). Unfortunately there were several non-specific bands, and thus we could not unequivocally demonstrate by western blot analysis that all Nesprin 1 isoforms were ablated in our mutant mice. However, immunostaining of skeletal muscle isolated from Nesprin $1^{-/-}$ mice and wild-type littermates demonstrated that no Nesprin 1 protein was detectable in tissue from Nesprin $1^{-/-}$ mice (Supplementary Material, Fig. S1F). Taken together, our data suggest that we have successfully created a Nesprin 1 knockout mouse line (Nesprin $1^{-/-}$) in which all isoforms of Nesprin 1 containing the C-terminal SR region with or without KASH domain were deleted.

Absence of Nesprin 1 causes post-natal lethality and growth retardation

Nesprin $1^{-/-}$ pups were born in Mendelian ratios with similar body size compared with wild-type littermates (Fig. 1A). At post-natal day 1, some Nesprin $1^{-/-}$ pups appeared weak and had little detectable milk in their stomachs, presumably reflecting an inability to suckle, whereas others were indistinguishable from their wild-type littermates. Genotyping of 87 offspring from heterozygous breeders indicated that more than 60% of the Nesprin $1^{-/-}$ pups died between post-natal days 2 and 11 (Fig. 1B). Surviving mice in this age range had 20–25% lower body weight than their wild-type littermates, likely the result of decreased milk intake caused by muscle weakness (Fig. 1C). Growth retardation was even more pronounced at the age of 21 days, when the body weight of the knockout was 33% lower than that of their wild-type littermates (Fig. 1C and D). There were no differences in survival or body mass between sexes within the knockout pups. The body weights of Nesprin $1^{-/-}$ mice surviving beyond 3 months were more variable, but were not significantly lower than the body weights of their wild-type littermates (data not shown).

Histopathological abnormalities in muscle from adult Nesprin $1^{-/-}$ mice

Frozen sections from quadriceps, gastrocnemius (Gas) and triceps muscles from Nesprin $1^{-/-}$ and wild-type littermate controls at 3 months of age (two males and two females from each group) were evaluated histologically and histochemically (Fig. 2A). No changes in myofiber size, fiber-type distribution or amounts of connective tissue were found in knockout mouse muscle compared with wild-type. Neither necrotic nor

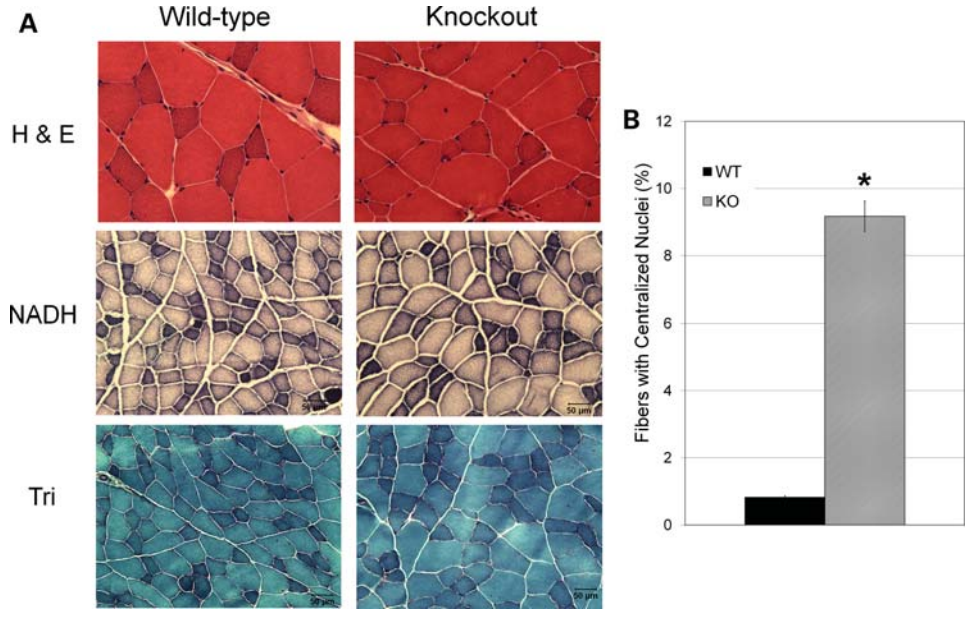

Figure 2. Histological and histochemical analyses of Nesprin $1^{-/-}$ mice. (**A**) Histological analysis: H&E and trichrome stains of representative fresh frozen gastrocnemius muscle of Nesprin $1^{-/-}$ mice and wild-type littermates. Fiber-type distribution was evaluated by NADH-dehydrogenase reaction. Type 1 fibers are dark blue and type 2 fibers are intermediate (type 2A) or light blue (type 2B). The only pathological abnormality identified in knockout muscle was the excessive numbers of centrally located nuclei. Bar = 50 μm for all figures. (**B**) Quantification of centralized nuclei in gastrocnemius muscle. In knockout muscle, 9% of the fibers contained centralized nuclei compared with less than 1% in wild-type muscle. $^{*}P < 0.0005$, $n \geq 5000$.

regenerating fibers were observed. However, the number of myofibers containing centralized nuclei was increased in all knockout mouse muscles analyzed and ranged from 5 to 12% compared with less than 1% in wild-type (Fig. 2B).

Nuclear positioning is defective in skeletal muscle fibers of Nesprin $1^{-/-}$ mice

To study the role of Nesprin 1 in nuclear positioning, we examined the spacing and location of nuclei in skeletal muscle fibers from the tibialis anterior (TA) muscle of 1-day-old and 4-month-old mice. Nuclei in wild-type fibers were evenly distributed across the width of the fiber and were not in close proximity to each other. On the other hand, nuclei in knockout fibers were often situated very close together, either in clusters or in lines along the length of the fiber (Fig. 3A and B). In addition, no clusters of synaptic nuclei were observed in the mutant muscle (data not shown). These observations are in agreement with the published observations of the other two Nesprin 1 mutant mice (24,25).

In skeletal muscle fibers from TAs of 4-month-old mice, quantification of clusters and lines of nuclei revealed that 40% of the nuclei in knockout fibers were part of a cluster and 11% nuclei were part a line (Fig. 3C). The remaining nuclei were irregularly spaced throughout the fiber, separate from one another. In wild-type littermates, less than 1% of nuclei outside of the neuromuscular junction were in clusters and no lines of nuclei were found.

Nuclear anchorage is disrupted in skeletal muscle fibers from Nesprin $1^{-/-}$ mice

Since previous studies revealed defective nuclear mechanics in Lamin-A/C-deficient cells, we investigated the nuclear mechanics in muscle fibers of Nesprin $1^{-/-}$ mice (30). In our first preparations of Nesprin $1^{-/-}$ glycerol-treated single fibers for nuclear mechanics testing, we observed a dramatic decrease in the number of nuclei that could be studied. Adult TA muscles were incubated for at least 48 h in a glycerol-based storage solution at -20°C to remove the sarcolemma, then single fibers were isolated and either immediately mounted on slides or subjected to a series of washes in bovine serum albumin (BSA)-based solutions at 4°C prior to mounting. Surprisingly, few nuclei remained attached in the unwashed Nesprin $1^{-/-}$ fibers, and almost no nuclei remained attached after washing, whereas in wild-type fibers, the nuclei remained attached to the myofiber (Fig. 4A, B and D). We confirmed that nuclear number was the same for wild-type and knockout fibers without glycerol treatment by counting nuclei in fibers isolated from fixed TA muscles (data not shown). To investigate this phenomenon further, we examined single fibers from muscles after only 12 h of incubation in storage solution. After the shorter incubation time, the sarcolemma was still partially intact, but had already detached from the myofibers. In knockout fibers, almost all of the nuclei had detached from the fibers along with the sarcolemma (Fig. 4C). In contrast, the nuclei were still completely secured to the wild-type myofibers (data not shown).

No difference in nuclear shape or perinuclear space in Nesprin $1^{-/-}$ mouse muscle

The first 10 nuclei (range 9–13) from cardiac and skeletal (Gas) muscles from three adult mice of each genotype (wild-type and Nesprin $1^{-/-}$) were photographed at $\times 10$–20 000 magnification. Negatives were first examined for evidence of an expanded perinuclear space, then for heterochromatin clumping and finally for marginal nuclear membrane profile. Ignoring

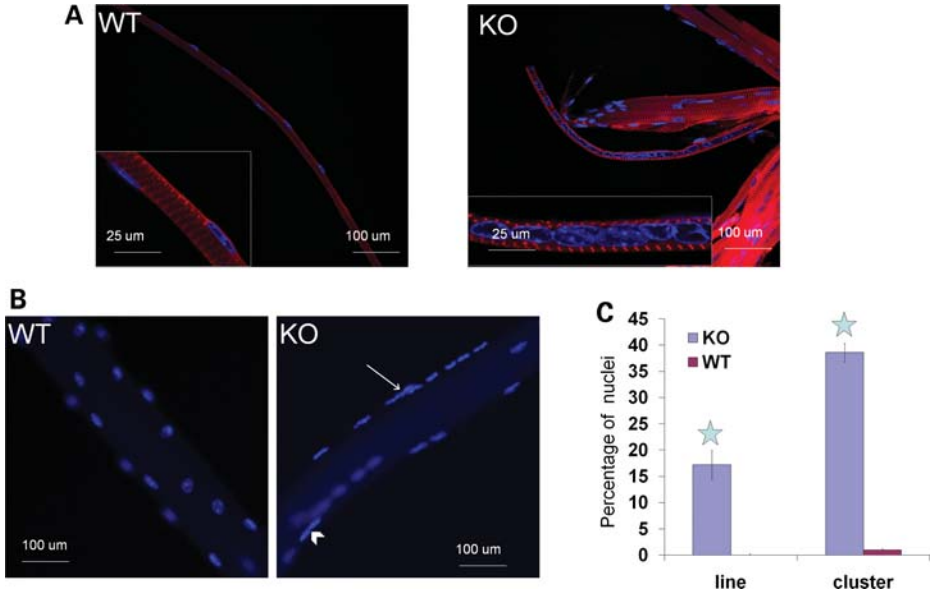

Figure 3. Nuclear positioning defects Nesprin $1^{-/-}$ mice. (**A**) Longitudinal images of single muscle fibers from 1-day-old mice. Fibers were isolated from fixed TA muscles and stained with α-actinin antibody (red) and DAPI (blue). Note clumping of nuclei in knockout fibers compared with the evenly spaced nuclei in wild-type fibers. Insets are higher magnification of regions of the main image. (**B**) Epifluorescence images of single fibers from fixed adult TA muscle, stained with DAPI. A 'line' of nuclei was defined as more than three nuclei strung together, and an example is indicated by the arrow. A cluster of nuclei was defined as 2–3 nuclei very close together. The arrowhead indicates a cluster. (**C**) Quantification of nuclear position defects. The percentages of nuclei included in either lines or clusters were determined from images of DAPI-stained fibers from fixed adult TA muscle. $^{*}P < 0.0005$, $n = 5$ mice.

nucleoli, heterochromatin was considered clumped if the normal marginal distribution just beneath the internal nuclear membrane was directed inward. The marginal nuclear membrane profile was considered abnormal if the membrane was excessively invaginated or crenated versus smooth, as in wild-type mice. When compared with wild-type nuclei, there was no difference in perinuclear space, distribution of heterochromatin or in the marginal nuclear membrane profile in cardiac or skeletal muscle from Nesprin $1^{-/-}$ mice (data not shown).

Minor changes in protein levels of Nesprin 1 binding partners in Nesprin $1^{-/-}$ tissue

To investigate whether expression levels of nuclear membrane proteins were altered in knockout mice, we performed western blot analyses of cardiac and skeletal muscle tissue from Nesprin $1^{-/-}$ and wild-type neonatal and adult mice. Blots were probed for Emerin, Lamin A/C, Lamin B1, Lamin B2, SUN1 and SUN2, as well as GAPDH as a loading control. This revealed upregulation of SUN1 in 1-day-old knockout heart as well as upregulation of SUN2 in 1-day-old knockout skeletal muscle but all other tested proteins remain unchanged in either 1-day-old knockout hearts or skeletal muscle (Fig. 5). No changes in expression levels of the tested proteins, Emerin, Lamin A/C, Lamin B1, Lamin B2, SUN1, SUN2 or Desmin were found between wild-type and knockout tissues from adult mice (data not shown).

Nesprin $1^{-/-}$ muscle fibers exhibit abnormal nuclear mechanics

Nuclear morphology and location only provide information regarding nuclear placement and structure. In order to investigate the degree of strain transmission between myonuclei and the cytoskeleton, we imaged the nuclei of knockout and wild-type single fibers during controlled deformation. The extent of fiber stretch was determined from the sarcomere length, which was measured based on immunolabeling of α-actinin, the prominent Z-disk protein. After fiber stretch over a similar sarcomere length range, both knockout and wild-type nuclei deformed linearly, but knockout nuclei deformed significantly less compared with wild-type nuclei (Fig. 6A). Nuclear aspect ratio (length divided by width) was calculated from the images at each stretch increment and normalized to initial aspect ratio. In knockout fibers, nuclear aspect ratio changed significantly less with increasing sarcomere length compared with wild-type fibers (Fig. 6B and C), indicating decreased strain transmission from perinuclear regions to the knockout nuclei.

Physiological function of skeletal muscle of Nesprin $1^{-/-}$ mice

Stress generation capacity of skeletal muscle from neonatal and 4-month-old Nesprin 1 knockout mice and their wild-type littermates was tested as described previously (31,32). Isometric stress tended to be lower at both ages, but the trend was not significant (Supplementary Material, Fig. S3A and B). In order to impose even higher stresses upon the muscles, isolated muscles from adult mice were also subjected to a bout of 10 eccentric contractions (ECs) after the initial isometric contractions. Stress generation declined during and after the bout for both genotypes, but there were no significant differences in either post-eccentric isometric stress or percent isometric stress drop (Supplementary Material, Fig. S3C). Nesprin $1^{-/-}$ muscles, however, did exhibit more variation in stress generated.

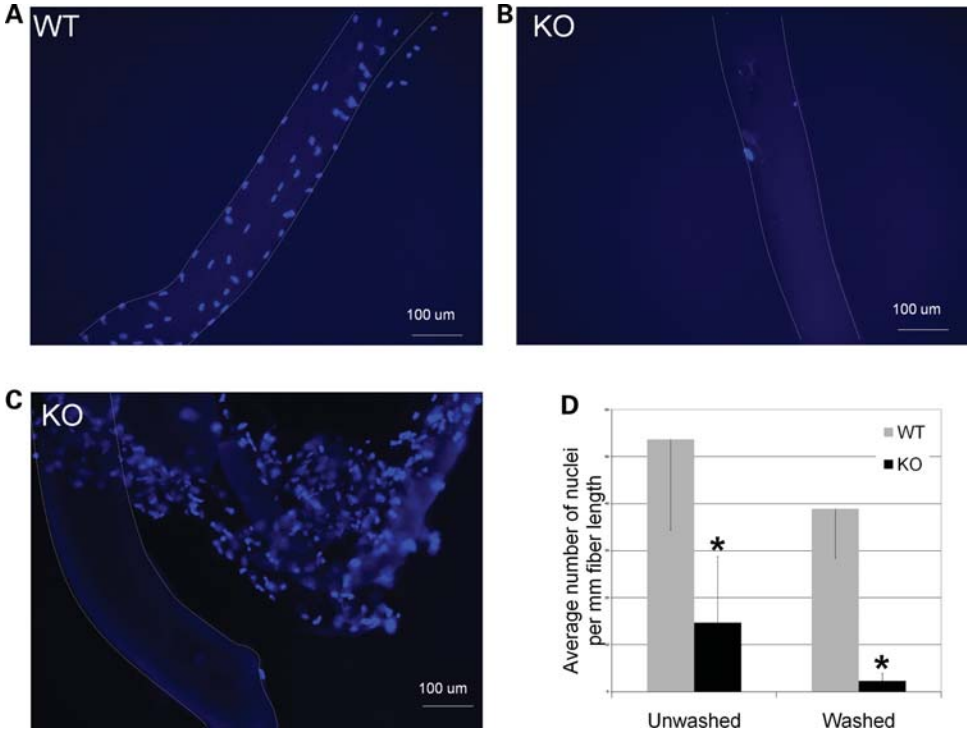

Figure 4. Nuclear anchorage defects. (**A** and **B**) Single fibers from muscles after a long incubation in glycerol-based storage solution which causes the sarcolemma to peel off muscle fibers. Fresh TA muscles were stored in a 50% glycerol storage solution at −20°C for at least 48 h to dissolve the sarcolemma. After incubation, single fibers were dissected out and subjected to a series of washes in BSA-based solutions at 4°C, then mounted on a slide with DAPI-containing mounting media. Dashed white lines delineate the outline of the fibers. In wild-type fibers, nuclei are still attached to the myofiber (A), whereas almost no nuclei remained attached to the myofibers from Nesprin $1^{-/-}$ muscles (B). (**C**) Single fiber from knockout muscle briefly incubated in glycerol. TA muscles were stored in 50% glycerol storage solution at −20°C for only 12 h before dissection of single fibers. In single fibers from wild-type muscle, the membrane was still intact, but had detached from myofibers, while the nuclei remained attached to the myofibers (data not shown). In knockout muscle, nuclei detached from the fibers along with the membrane. They can be seen embedded in the still-intact membrane. (**D**) Quantification of nuclear detachment in glycerol-treated muscle. After a long incubation in storage solution and single fiber dissection, some fibers were immediately mounted on slides with DAPI (unwashed group), whereas others underwent a series of washes beforehand (washed group). Error bars indicate standard deviations. $^{*}P < 0.0005$ between wild-type and knockout both for washed and unwashed groups. Washed $n = 6$ mice, unwashed $n = 19$ mice.

Reduced exercise capacity in Nesprin $1^{-/-}$ mice

Adult wild-type and Nesprin $1^{-/-}$ mice were subjected to daily treadmill running over a 3-week period. Average distance run (Supplementary Material, Fig. S3D) and average running time (data not shown) were both significantly lower for knockout mice compared with wild-type at 7, 14 and 21 days into exercise training.

Nesprin $1^{-/-}$ mice have normal heart function

To elucidate the underlying basis for differences in exercise capacity between genotypes, we studied the heart function of Nesprin $1^{-/-}$ mice by echocardiogram and electrocardiogram. We tested five pairs of Nesprin $1^{-/-}$ mice and wild-type littermates within the following four groups: males and females at 3, 6, 9 and 12 months of age. Parameters measured included heart rate, left ventricle mass, left ventricle internal end-diastolic dimension, left ventricle systolic dimension, left ventricle fractional shortening, left ventricle wall thickness (diastolic and systolic), PR interval and QRS duration. We did not find any significant change in these cardiac function measures between Nesprin $1^{-/-}$ mice and wild-type littermates as a function of either gender or age (data not shown).

Existence of Nesprin 1 splicing isoforms without the KASH domain in mouse brain

Over 60% of our Nesprin $1^{-/-}$ mice died perinatally, which is similar to the survival rate of Nesprin 1 mutant mice generated by Puckelwartz *et al*. (25), but in contrast to the normal viability of Nesprin 1 mutants generated by Zhang *et al*. (24). Detailed analysis of the targeting strategies utilized by the three laboratories to generate the mutant mice revealed that, owing to remaining alternative splicing sequences, Nesprin 1 splicing isoforms without the KASH domain (26) may be still intact in mutant mice generated by Zhang *et al*. (24), whereas the Nesprin 1 splicing isoforms without the KASH domain would be ablated in mutants generated by Puckelwartz *et al*. (25) and in our Nesprin 1 mutants (Supplementary Material, Fig. S2). We investigated whether there are normally mouse Nesprin 1 transcripts lacking the penultimate exon that give rise to splicing isoforms without the KASH domain, as in humans (26). RT–PCR analysis of exon inclusion in Nesprin 1 transcripts was performed on RNA from the following different organs: brain, heart, kidney, liver, lung, skeletal muscle and spleen (Fig. 7). A truncated Nesprin 1 transcript was found in the brain. Sequencing confirmed that the second-to-last exon was skipped. The skipping of the

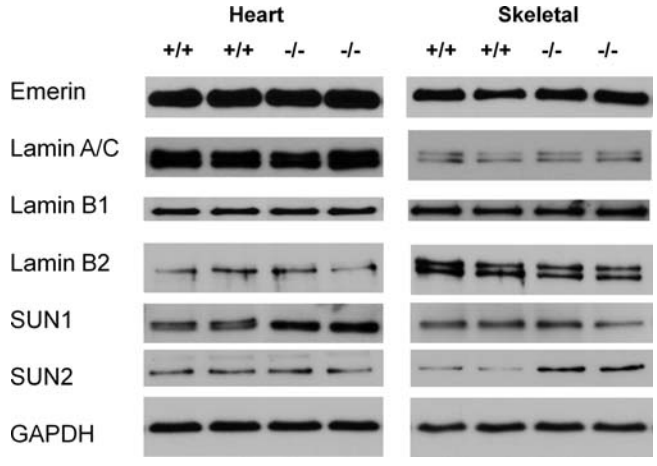

Figure 5. Western blot analysis of neonatal day 1 cardiac and skeletal muscle for INM proteins. In knockout hearts, SUN1 levels are upregulated compared with wild-type, and in skeletal muscle, SUN2 levels are upregulated compared with wild-type. The levels of other INM binding proteins are similar between genotypes in both cardiac and skeletal muscle.

penultimate exon leads to a novel transcript which includes an 11 novel codons followed by a stop codon, to result in a putative translation product lacking the KASH domain (Supplementary Material, Fig. S2).

DISCUSSION

We successfully created a Nesprin 1 knockout mouse line (Nesprin $1^{-/-}$) in which all isoforms of Nesprin 1 containing the C-terminal SR region with or without KASH domain were ablated. We found that young Nesprin $1^{-/-}$ mice of both sexes experienced growth retardation, increased variability in body weight and decreased exercise tolerance compared with wild-type animals.

Previous models used to study Nesprin 1 have included Nesprin $1^{\Delta KASH}$ mice, in which only the KASH domain of Nesprin 1 was deleted (24) and Nesprin 1^{rKASH} mice, in which the KASH domain of Nesprin 1 was replaced by an unrelated sequence of 61 amino acids (25). In both Nesprin $1^{\Delta KASH}$ and Nesprin 1^{rKASH} mutant mice, mutant Nesprin 1 proteins are still expressed, whereas our mutant mice are null mutants (Supplementary Material, Fig. S2). Our results confirm that Nesprin 1 is crucial for normal survival and growth. Over 60% of our Nesprin $1^{-/-}$ mice died perinatally, which is similar to the survival rate of the Nesprin 1^{rKASH} mice (25), but in contrast to the normal viability of the Nesprin $1^{\Delta KASH}$ line (24). Nesprin 1 transcripts lacking the penultimate exon, which give rise to splicing isoforms without the KASH domain, have previously been found in human tissues (26). We identified a Nesprin 1 isoform lacking the penultimate exon in mouse brain. The truncated isoform(s) would be intact in the Nesprin $1^{\Delta KASH}$ mice (24) since the authors only partially ablated the last exon, leaving the splicing site of the last exon intact (Supplementary Material, Fig. S2). However, the truncated isoform should be ablated in both Nesprin 1^{rKASH} and our mutant mice (Supplementary Material, Fig. S2). Thus, ablation of Nesprin 1 isoforms without KASH domain, in addition to ablation of other KASH domain-containing isoforms, might cause the partial post-natal lethality observed in Nesprin 1 mutants generated by Puckelwartz *et al*. (25) and by our group. Future studies are needed to unequivocally demonstrate this. Nesprin $1^{\Delta KASH}$–Nesprin $2^{\Delta KASH}$ double mutants that lack the KASH domains of both Nesprins 1 and 2 but have the splice sites required to generate KASH-less isoforms (24) display 100% perinatal lethality, suggesting that in this situation, lethality results from loss of only KASH-containing isoforms.

We observed that young Nesprin $1^{-/-}$ mice of both sexes experienced growth retardation and increased variability in body weight, while it was reported that only the female Nesprin 1^{rKASH} mice had delayed growth. We did not observe any other overt changes in the Nesprin $1^{-/-}$ mice such as the kyphoscoliosis or poor grooming that were seen in the Nesprin 1^{rKASH} mice (25). The differences in phenotype could be caused by the different knockout strategies employed (Supplementary Material, Fig. S2) and/or the differences in the genetic backgrounds.

In agreement with the previous studies, we showed that Nesprin 1 is important for the proper localization of skeletal muscle nuclei. Specifically, we found that 50% of all myonuclei in Nesprin$^{-/-}$ muscle fibers were either clustered or in a linear array. Similarly, in the Nesprin $1^{\Delta KASH}$ mice, 99% of fibers were observed to contain three or more nuclear clusters (24). Non-synaptic nuclei of Nesprin 1^{rKASH} muscles were also abnormally distributed along the length of the fiber (25). Cross-sections revealed non-peripheral nuclei in 9% of Nesprin $1^{-/-}$ muscle fibers, which is similar to the 14% of muscle fibers with non-peripheral nuclei found in muscle cross-sections from Nesprin 1^{rKASH} mice (25).

When expression levels of INM membrane proteins were examined, we found only minimal changes: SUN1 and SUN2 were upregulated in neonatal Nesprin $1^{-/-}$ cardiac and skeletal muscle, respectively. The near-normal protein levels were surprising considering the abnormalities found in nuclear attachment and mechanics, but were similar to the results found by immunostaining of muscle tissue from Nesprin 1^{rKASH} mice for proteins in the LINC complex (25). Since there is a high degree of homology between the KASH domains of Nesprins 1 and 2, it is likely that Nesprin 2 maintains near-normal localization and quantities of these proteins in the absence of Nesprin 1.

In contrast to the abnormally compliant nuclei of Lamin-A/C deficient cells (33), nuclei of Nesprin $1^{-/-}$ single muscle fibers exhibited less stretch than wild-type nuclei when strain was applied to the fibers following permeabilization with Triton X-100 (0.1%). The difference is indicative of the distinct roles of Lamin-A/C and Nesprin 1. While Lamin-A/C serves to stabilize and strengthen the nuclear envelope, Nesprin 1 serves as a link between the nuclei and the cytoskeleton. Our experiments show that Nesprin 1 is essential for proper strain transmission from the cell to the nucleus in muscle. In similar studies performed on muscle fibers from desmin$^{-/-}$ mice, strain transmission between fiber and nuclei was also found to be defective, with nuclei from the desmin-null fibers stretching less than the nuclei from wild-type fibers (34). This finding is consistent with our current work, as desmin is the main component of the myofiber intermediate filament cytoskeleton, which is linked to the nucleus via the Nesprin 3–plectin–desmin interaction (7).

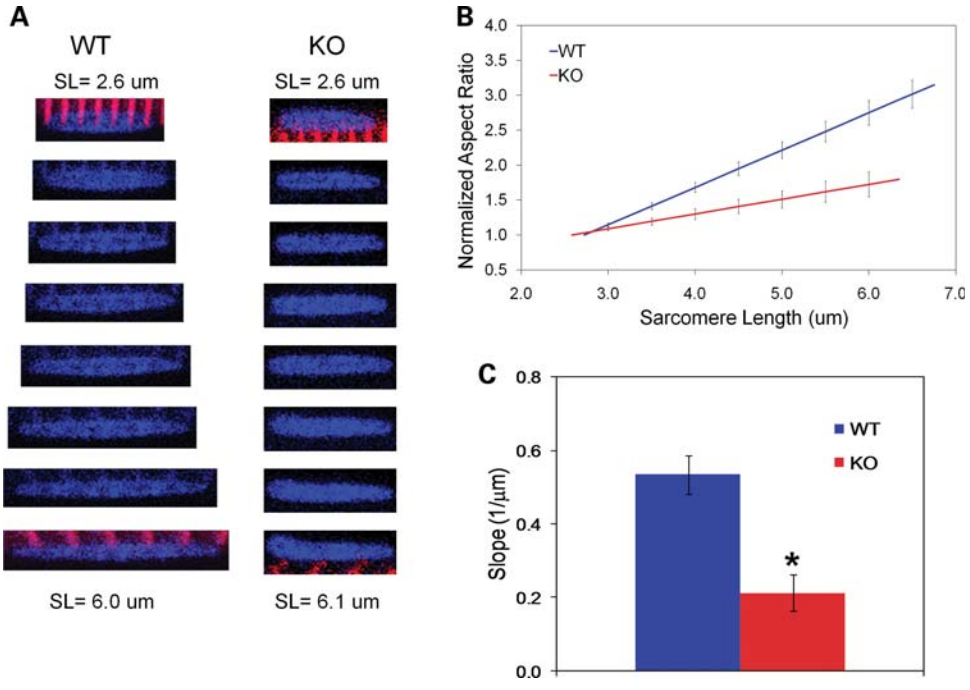

Figure 6. Nesprin $1^{-/-}$ muscle fibers exhibit abnormal nuclear mechanics. (**A**) Nuclear elongation during stretch of single fibers. Single fibers were dissected from TA muscles after incubation in 0.1% Triton X-100. Fibers were mounted on a custom setup, stained with α-actinin antibody (red) and nuclear label (blue) and were imaged under a confocal microscope during incremental stretches. Wild-type nuclei appear to stretch more with fiber strain compared with knockout nuclei. Sarcomere length (SL) was measured based on α-actinin staining and was used as a measure of fiber strain. (**B**) Change in the normalized nuclear aspect ratio with sarcomere length. The trend line is the average of the line fits to the data points from each experiment. Wild-type, blue; knockout, red. Nuclear aspect ratios were normalized to their starting value at the initial fiber length. (**C**) The nuclear aspect ratio changed less with fiber strain in knockout fibers compared with wild-type fibers. The bars represent the slope of the trend lines shown in (B). $^{*}P < 0.0003$, $n = 11–12$.

We also report that mice lacking Nesprin 1 have significantly decreased exercise capacity. However, muscle stress production, susceptibility to EC-induced injury and cardiac electrophysiology were not different between wild-type and knockout mice. Nesprin $1^{-/-}$ mice did not have the cardiac conduction system defects and prolonged PR intervals reported for the Nesprin 1^{rKASH} mice (25). Again, this difference in observed phenotypes could be caused by the different targeting strategies employed but precise underlying mechanisms are not yet known. One reason that the Nesprin $1^{-/-}$ mice might have decreased exercise capacity, despite having normal muscle stress production and normal heart function, might be compromised motor neuron development. Poor motor control would lead to less efficient patterns of movement, and thus a lower exercise capacity even when the muscles have the same stress generation capabilities. Although we did not specifically investigate motor control in this study, nor did we notice any obvious signs of motor dysfunction, it has been previously reported by Puckelwartz *et al*. (25) that female Nesprin $1^{\Delta KASH}$ mice are less coordinated than their wild-type controls.

A striking phenotype observed in the Nesprin 1 knockout is the distinctive decrease in the number of nuclei remaining attached to glycerol-treated Nesprin $1^{-/-}$ fibers compared with glycerol-treated wild-type fibers. Desmin also supplies a mechanical linkage between the nuclei and the cytoskeleton (34) and is thought to connect Nesprin 3 to the ONM via Plectin (7). Upon treatment with glycerol-based storage solution, however, nuclei from desmin$^{-/-}$ muscles remained attached to the myofibrils, indicating that nuclear attachment to the myofibrils is mediated through proteins other than Nesprin 3 and Desmin (Fig. 8). In the current study, we found that without the presence of an intact sarcolemma, the nuclei are no longer associated with the cytoskeleton in Nesprin $1^{-/-}$ mice. Thus, we propose that Nesprin 1 forms the critical link between the nucleus and the myofibers, without which nuclear attachment to myofibers is completely abolished (Fig. 8).

A basic question relevant to all cell biology is how the nucleus is connected to the rest of the cell. The importance of the mechanical integration of the cell membrane, cytoskeleton and nuclei has been the topic of several recent reviews (35–37). Many of the muscular dystrophies seem to result from defects in the proteins that supply this mechanical connection. One specific example pertaining to nuclear mechanics is that 40% of EDMD patients have mutations in either Emerin or LMNA, two components of the nuclear LINC complex (2). LMNA has been shown to be critical in maintaining normal nuclear mechanics (38), and mice lacking LMNA exhibit many of the features of EDMD (39). Additionally, fibroblasts lacking Emerin or Lamin A have nuclear shape abnormalities similar to fibroblasts from EDMD patients, and a drastically altered signaling response to mechanical stretch (30). Finally, myoblast differentiation is impaired in cells lacking either Emerin or LMNA (40,41). Approximately 60% of EDMD patients do not have mutations in Emerin or LMNA, which is especially interesting in light of a recent study suggesting that mutations in Nesprins 1 and 2 are involved

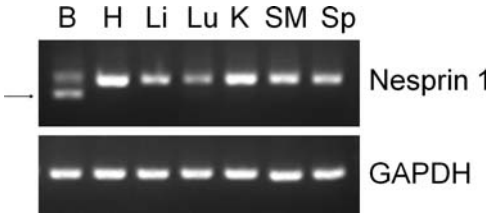

Figure 7. Alternative tissue-specific splicing of Nesprin 1 transcripts. RNA was isolated from brain (B), heart (H), liver (L), lung (Lu), kidney (K), skeletal muscle (SM) and spleen (Sp) and reverse-transcribed to cDNA. PCR yielded two bands in brain and only one band in the other tissues. The additional lower band indicates that a Nesprin 1 isoform without the KASH domain is normally produced in the brain.

in the pathogenesis of EDMD (3). Knockdown of Nesprin 1 or 2 in fibroblasts mimicked the nuclear defects and Emerin mislocalization seen in fibroblasts from EDMD patients (3). While nuclear ultrastructure of the Nesprin $1^{-/-}$ skeletal muscle did not differ from wild-type muscle, abnormal nuclear mechanics was observed. Further studies of the role of Nesprins 1 and 2 in skeletal myoblast differentiation, nuclear stiffness and mechanotransduction may help elucidate the role of the Nesprins in the disease mechanism of EDMD.

MATERIALS AND METHODS

Gene targeting and generation of Nesprin 1 knockout mice

Nesprin 1 genomic DNA was isolated from a R1 ES cell and was used to create a Nesprin 1-targeting construct containing *flox*P sites and the *neomycin* resistance gene. The construct was generated in the pBluescript II KS+ vector, and the 5′ arm of homology consisted of a 2.75 kb *Not*I–*Sal*I fragment fused with first *flox*P site upstream of Nesprin 1 exon 16 followed by *neomycin* flanked by *FRT* sites. The 3′ arm of homology was a 2.92 kb *Sal*I–*Kpn*I fragment located downstream of second *flox*P site (Supplementary Material, Fig. S1A). The targeting construct was verified by sequencing and linearized with *Not*I before electroporation into R1 ES cells at the Transgenic Core Facility at the University of California, San Diego. Seven hundred G418-resistant ES clones were screened for homologous recombination by Southern blot analysis as described in the following section.

Southern blot analysis

Genomic DNA was extracted from G418-resistant ES cell clones and mouse tails as previously described (42). ES cell DNA was digested with *Hin*dI and analyzed by Southern blot analysis. A 535 bp fragment was generated by PCR using mouse genomic DNA and specific Nesprin 1 primers (forward, TATACCATCAGGATTGGTTTCATTGG; reverse, ACTACGTCCTGGTCCAGGAAACATG). The PCR product was subsequently radiolabeled using α-[^{32}P]dCTP by random priming (Invitrogen). DNA blots were hybridized with the radiolabeled probe and visualized by autoradiography. The wild-type allele is represented by a band of 9.2 kb, whereas a band of 5.2 kb represents the correctly targeted mutant allele.

Generation and genotyping of mice

Two independent homologous recombinant ES clones were microinjected into blastocysts from C57/B6 mice at the Transgenic Core Facility at the University of California, San Diego. Male chimeras were inbred with female Black Swiss mice to generate germ line-transmitted heterozygous mice (Nesprin $1^{+/-}$). Nesprin $1^{+/-}$ mice were subsequently intercrossed to generate homozygous null mutant mice (Nesprin $1^{-/-}$).

Offspring were genotyped by PCR analysis using mouse tail DNA and wild-type (forward, TGGTAGTCATCAAGATG CTGGCTTGGG; reverse, CTTTCTAAGTCTACAGTGGT GGGCTC) and knockout allele-specific primers (forward, GT AATATTTGTGGGACCGAGTTCTCTGAG, reverse primer is the same as wild-type).

Total protein extracts were prepared from post-natal TA muscle separated on a 4–15% Ready Tris–HCl gel (BioRad) and subjected to western blot analysis using polyclonal antibody against sequence 841-GRSTPNRQKSPRGKC-855 from Nesprin 1α (synaptic nuclear envelope 1 isoform 2, NP_071310.2). Glyceraldehyde-3-phosphate dehydrogenase (GADPH) antibody was used for normalization (1:10 000, Sigma-Aldrich).

Single fiber isolation and staining

To obtain a large number of fine single myofibers, TA muscles were fixed with 4% paraformaldehyde (PFA) for more than 2 days. Fixed muscles were divided into several bundles by pulling the tendon with tweezers, and non-muscle tissue was removed to the greatest degree possible under a binocular microscope. The muscle bundles were macerated in 40% NaOH solution for 3 h at room temperature and then shaken for 5–10 min to separate the bundle into single myofibers. Isolated myofibers were rinsed twice with phosphate-buffered saline (pH 7.3) for neutralization. They were then mounted in mounting medium with DAPI (Vector, H1200).

Myofibers were also isolated from glycerol-extracted muscle: TA muscles were dissected from the bone and soaked overnight in 50% glycerol diluted with calcium-chelated saline at 4°C, and the myofibers were then mechanically isolated from the muscle tissue with sharpened fine tweezers under a dissecting microscope. These mechanically isolated single myofibers were also fixed with calcium-chelated 4% PFA before being mounted on a glass slide in mounting medium with DAPI (Vector, H1200).

RT–PCR

Total RNA was extracted from 1-month-old wild-type mouse tissues using a standard Trizol RNA isolation protocol (Invitrogen). The first strand was generated by SuperScript First Strand Synthesis System (Invitrogen). PCR was performed using primers located in the third-from-last and last exon (P1, GTCCCACATCCGGAAGAAGTACCCC and P3, CTT CAGAGTGGAGGAGGACCGTTGG) and 17th and 13th exon (P17, GAGAACAAAATCCAGCTTCAGGAAAT GGGAG and P13, GTAGGTCGTCCCATCTCTGGTTGCC). The amplified samples were run on an agarose gel and the results were confirmed by sequencing.

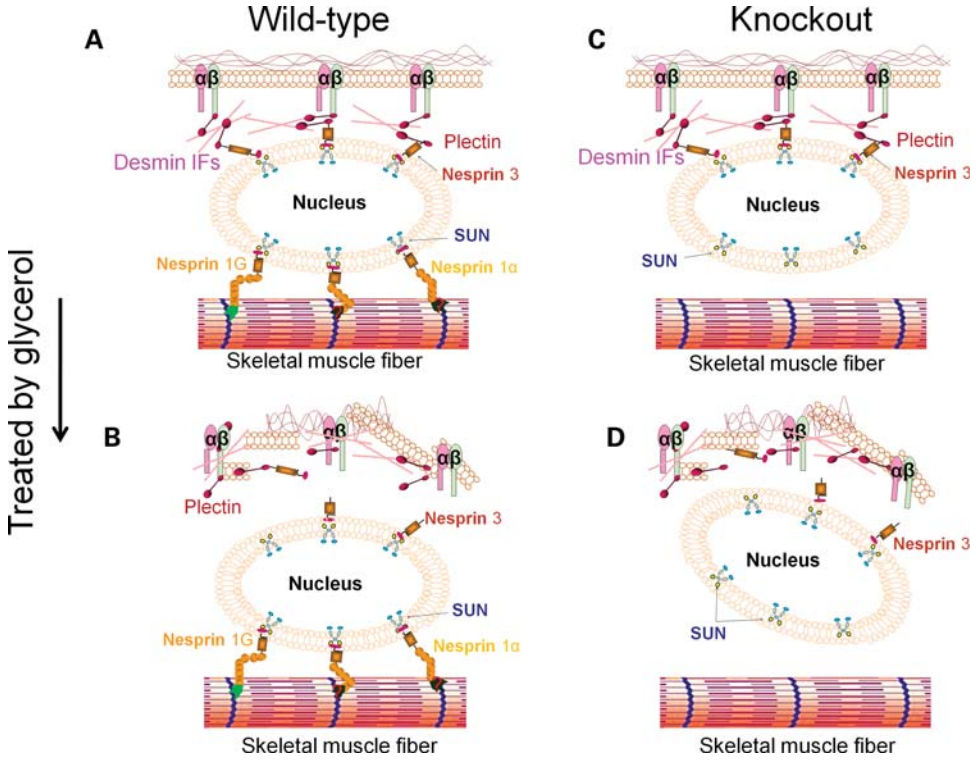

Figure 8. Model of Nesprin 1-mediated nuclear attachment. (**A**) Wild-type myofiber. Nuclei are attached to both the cell membrane and myofibrillar actin. The attachment to actin is likely mediated by Nesprin 1G and other splice isoforms and may involve an unknown protein(s). Symbol '?' represents unknown molecule(s) linking Nesprin 1 alpha to actin filaments. (**B**) Wild-type fibers after glycerol treatment. The cell membrane is permeablized, but the nuclei remain in place because of their attachment to actin via Nesprin 1. (**C**) Nesprin 1 knockout myofiber. Nuclei are no longer attached to myofibrillar actin, but remain in place via their connections to the cell membrane. (**D**) Nesprin 1 knockout myofibers after glycerol treatment. The nuclei are no longer connected to the myofibers and are washed away from the fibers once the cell membrane is no longer intact.

Immunostaining

Hindlimbs from post-natal day 1 mice were fixed overnight in 4% PFA in either an unstretched or stretched position as described by Bang *et al*. (43). The TA was dissected out and incubated in 10, 15 and 30% sucrose in PBS before freezing in optimal cutting temperature. Ten micrometer cross frozen sections were permeabilized and blocked in 5% normal goat serum, 0.3% Triton X-100, 5% BSA (Sigma-Aldrich) in 1× PBS for 2 h, followed by incubation overnight at 4°C in a humidified chamber with sarcomeric α-actinin antibody (1:500; Sigma-Aldrich) in blocking buffer. After rinsing in wash buffer (1×PBS with 0.3% Triton X-100), sections were incubated at room temperature for 2 h with fluorescently labeled secondary antibodies (1:100 goat anti-mouse cy3) in blocking buffer. Slides were rinsed in wash buffer and mounted in mounting buffer with DAPI (Vector Laboratory, H1200).

In the adults, TA muscles were dissected and frozen in isopentane pre-cooled in liquid nitrogen for 45 s and then stored at −80°C. Cryostat sections (10 μm) were cut and fixed by acetone at −20°C for 10 min. After permeabilization with washing buffer, slides were blocked in blocking buffer described in previous section for 2 h and then incubated with the following antibodies: anti-SUN1 (1:150, kindly provided by Dr Sue Shackleton, University of Leicester, University Road, UK), anti-SUN2 (1:100, kindly provided by Dr Didier Hodzic, Washington University School of Medicine, St Louis, MO, USA), anti-Lamin A/C (1:1000, kindly provided by Dr Larry Gerace, Scripps Research Institute, La Jolla, CA, USA), anti-Nesprin 1 (1:100), anti-Emerin (1:100, Santa Cruz) and anti-Desmin (D33; 1:25; Sigma-Aldrich). After rinsing in wash buffer, sections were incubated at room temperature for 2 h with fluorescently labeled secondary antibodies (1:100 goat anti-mouse cy3, 1:100 goat anti-rabbit cy2 or cy3, 1:50 goat anti-guinea pig FITC) and DAPI in blocking buffer. Finally slides were mounted in mounting media (Dako S3023). Confocal microscopy was performed using a confocal microscope (FluoView, Olympus) with a 40× (NA 1) plan-apochromat oil objective. Individual images (1024 × 1024 dpi) were converted to tiff format and merged as pseudocolor RGB images using ImageJ (NIH).

Exercise

Six pairs of 4-month-old Nesprin $1^{-/-}$ mice and wild-type littermates were subjected to 3 weeks of daily treadmill exercise (Model: Exer-6M Treadmill with Treadmill Shock Detection Unit). Mice were placed in their respective lanes with the shocking apparatus turned off and allowed to adjust to the surroundings for 15 min. During the adjustment period, the treadmill was set to 0.3 m/s, and the mice were trained to run with gentle prodding for 2 h every day. The treadmill incline was

set to 25° at all times. Exercise capacity was assessed by daily treadmill run to exhaustion. At regular intervals, the speed of the treadmill was ramped up every 3 min from the initial 0.23 to 0.32 m/s in 0.03 m/s steps. Then the speed was increased from 0.35 to 0.41 m/s in 0.03 m/s steps every 20 min. The speed was then returned to 0.35 m/s and held there until exhaustion, defined as inability to continue running despite gentle prodding.

Histopathology and ultrastructural analysis

Muscle specimens (cranial tibial, Gas, quadriceps and triceps) from 4-month-old knockout and wild-type mice were collected immediately following euthanasia. Specimens were flash frozen in isopentane pre-cooled in liquid nitrogen and stored at −80°C until further processed. Cryostat sections (8 μm) were cut then stained by a standard panel of histochemical stains and reactions (44). Additional muscle specimens were immersion fixed in 5% glutaraldehyde in 0.1% phosphate buffer for 24 h. Following rinses, tissues were post-fixed in 1% aqueous osmium tetroxide for 3–4 h and then dehydrated in a graded alcohol series and propylene oxide. After infiltration with a 1:1 mixture of propylene oxide and araldite resin for 4 h, muscles were placed into 100% araldite resin overnight and then embedded in fresh araldite resin. Thick sections (1 μm) were cut with glass knives and stained with Toluidine blue prior to light microscopic examination. Thin sections (60–90 nm) were cut with a diamond knife and stained with uranyl acetate and lead citrate before examination in a Zeiss 10 electron microscope.

Skeletal muscle physiology

Studies of neonatal muscle stress generation were performed as described previously (32). The Gas muscles of 1-day-old Nesprin $1^{-/-}$ mice and their wild-type littermates were used for this study. Briefly, mice were sacrificed and hindlimbs were transected at the proximal femur, carefully skinned and immersed in ice-cold mammalian Ringer solution (137 mM NaCl, 5 mM KCl, 1 mM NaH_2PO_4, 24 mM $NaHCO_3$, 2 mM $CaCl_2$, 1 mM $MgSO_4$, 11 mM glucose and 10 mg/l curare). The Achilles tendon was released at its calcaneal insertion and the tibia and anterior muscle compartment were carefully resected to isolate the Gas and its origin on the distal femur. The Gas was transferred to a custom-made chamber filled with Ringer solution, which has been previously described (31). To secure the muscle in the chamber, the Achilles tendon was tied to a rigid post-interfaced with a force transducer (Series 300B, Aurora Scientific, Aurora, ON, Canada) using silk sutures. The femur was secured to a post-attached to a micromanipulator. The Gas muscle length (L_m) was adjusted such that passive muscle tension was barely detectable by the force transducer. Muscles were activated by an electrical stimulator (Pulsar 6 bp, FHC, Bowdoinham, ME, USA) via platinum plate electrodes that extended across the entire Gas length. Maximum isometric force was elicited by applying a 400 ms train of 0.3 ms supra-maximal pulses delivered at 100 Hz while maintaining constant L_m. A computer algorithm in LabVIEW (National Instruments, Austin, TX, USA) was used to trigger the stimulator, acquire signals from the force transducer via a data-acquisition board sampling at 4000 Hz (PCI-6040 m, National Instruments) and analyze force–time records. After being tested, the Gas was removed from the chamber, the Achilles tendon and femoral origin were cut off and the Gas was dabbed dry and weighed.

To determine the isometric stress generated, isometric force was normalized to physiological cross-sectional area (PCSA). For computations, previously published density and architectural values for the mouse Gas were used (32,45,46).

Studies of adult skeletal muscle physiology were performed as described previously (31). Mice were sacrificed and the fifth-toe belly of the extensor digitorum longus (EDL) muscle was dissected in mammalian Ringer solution. The 5th toe EDL was then transferred to a custom chamber filled with Ringer solution. Using 8-0 silk sutures, the muscle origin was secured by the tendon at a rigid post-attached to a micromanipulator and the insertion was secured by the tendon to the arm of a dual-mode ergometer (model 300B, Aurora Scientific). Sarcomere length was measured by laser diffraction at 632.8 nm and set to 3.0 μm. Muscle length (L_m) was defined as the tendon-to-tendon distance when at a sarcomere length of 3.0 um. The EDL muscle was subjected to three passive stretches, one every 2 min, each at 10% of L_m and at a velocity of $0.7L_m$/s. Maximum isometric tension was measured by applying a 400 ms train of 0.3 ms pulses delivered at 100 Hz while muscle length was held constant. This measurement was repeated twice more at 2 min intervals. The stimulation frequency chosen for these isometric contractions and the other contractions that follow was 100 Hz, as this frequency produced a fused tetanic contraction, but was low enough to prevent excessive fatigue. Selected muscles underwent 10 ECs, one every 2 min, each time stretched to 15% of L_m at the velocity of $2L_m$/s. Following the EC cycle, the isometric contractions were repeated three times at 2 min intervals. Muscle weight was measured to determine the PCSA (31). Data were acquired using a CA-1000 data board and analyzed in LabVIEW 7.0 (National Instruments).

Nuclear anchorage studies

Shortly after euthanization, TA muscles were dissected from hindlimbs and placed in a glycerol-based storage solution [consisting of (mM): KPropionate 170.0, K_3EGTA 5.0, $MgCl_2$ 5.3, imidazole 10.0, Na_2ATP 21.2, NaN_3 1.0, glutathione 2.5, 50 μM leupeptin and 50% (v/v) glycerol] at −20°C for at least 24 h but no more than 2 weeks. Single intact fiber segments were carefully dissected in relaxing solution [at pCa 8.0 and pH 7.1 consisting of (mM): imidazole 59.4, KCH_4O_3S 86.0, $Ca(KCH_4O_3S)_2$ 0.13, $Mg(KCH_4O_3S)_2$ 10.8, K_3EGTA 5.5, KH_2PO_4 1.0, Na_2ATP 5.1 and 50.0 μM of the protease inhibitor leupeptin]. Fibers were then either placed directly onto glass slides and mounted with DAPI-containing Vectashield (Vector Laboratories, Burlingame, CA, USA) (unwashed group) or were transferred to a chamber where the fiber segments were secured between two stationary wires with suture loops (washed group). Segments displaying abnormal discoloration, nicks or localized swelling were discarded. The fibers in the washed group were rinsed three times using relaxing solution with 1%

BSA, followed by incubation at 4–8°C with gentle agitation in 15 μl/ml normal horse serum in 0.1% BSA (15 min), 100 μl/ml normal mouse serum in 0.1% BSA (15 min) and 0.1% BSA (three washes of 5 min each). The fiber segments were then incubated with α-actinin antibody (Sigma A7811; St Louis, MO, USA) pre-conjugated to AF594 (Molecular Probes A-10239; emission = 594 nm) at 4°C overnight. After three more washes in 0.1% BSA (15 min each), fiber segments were mounted on slides with DAPI-containing Vectashield (Vector Laboratories). Slides were imaged at 10 or 20× with a Nikon Microphot-SA epifluorescent microscope (Nikon Instruments, Melville, NY, USA) and photographed with a SPOT digital camera (Diagnostic Instruments, Sterling Heights, MI, USA).

Nuclear stretch

Fibers to be used for nuclear stretch experiment were prepared in a similar way as the 'washed' fibers. While under anesthesia, the TA muscle was excised, then incubated in 0.1% Triton X-100 on ice for 2–4 h before proceeding with single fiber dissection. Single fiber segments were mounted in a chamber between a stationary post and a force transducer in a custom-built apparatus previously described (47). Fibers underwent the washes described above followed by an additional 30 min wash in 1.5 μl/ml DRAQ5, a far-red fluorescent DNA dye. The apparatus was then mounted on an inverted confocal microscope (LSM 510, Zeiss). Fibers were stretched just to the point where the passive force could be detected by the force transducer. At this point, the resting fiber length (L_o) was measured, the fiber diameter was measured in three different locations along the fiber, and a region of interest was identified and imaged. Fibers were then stretched in increments of 10% L_o and allowed to stress-relax for 2 min. At the end of each 2 min interval, passive force was recorded and a confocal image stack of the region of interest was taken.

Changes in nuclear shape with increasing stretch were determined from the DRAQ5 signal in the confocal images by fitting ellipses to the nuclei and recording the lengths of the major and minor axes in successive images. Sarcomere length was computed with a custom-written Matlab program from the α-actinin label in the confocal images.

SUPPLEMENTARY MATERIAL

Supplementary Material is available at *HMG* online.

ACKNOWLEDGEMENTS

We thank Drs Marie-Louise Bang and Angelika Anna Noegel for critical reading of the manuscript. Knockout mice were generated at the transgenic core facility at University of California at San Diego.

Conflict of Interest statement. None declared.

FUNDING

The work was supported by National Institutes of Health grants for Drs J.C. and R.L.L., and grants from the Muscular Dystrophy Association to Drs G.D.S. and S.L.

REFERENCES

1. Emery, A.E. (1989) Emery-Dreifuss syndrome. *J. Med. Genet.*, **26**, 637–641.
2. Bonne, G., Yaou, R.B., Beroud, C., Boriani, G., Brown, S., de Visser, M., Duboc, D., Ellis, J., Hausmanowa-Petrusewicz, I., Lattanzi, G. *et al.* (2003) 108th ENMC International Workshop, 3rd Workshop of the MYO-CLUSTER project: EUROMEN, 7th International Emery-Dreifuss Muscular Dystrophy (EDMD) Workshop, 13–15 September 2002, Naarden, The Netherlands. *Neuromuscul. Disord.*, **13**, 508–515.
3. Zhang, Q., Bethmann, C., Worth, N.F., Davies, J.D., Wasner, C., Feuer, A., Ragnauth, C.D., Yi, Q., Mellad, J.A., Warren, D.T. *et al.* (2007) Nesprin-1 and -2 are involved in the pathogenesis of Emery Dreifuss muscular dystrophy and are critical for nuclear envelope integrity. *Hum. Mol. Genet.*, **16**, 2816–2833.
4. Attali, R., Warwar, N., Israel, A., Gurt, I., McNally, E., Puckelwartz, M., Glick, B., Nevo, Y., Ben-Neriah, Z. and Melki, J. (2009) Mutation of SYNE-1, encoding an essential component of the nuclear lamina, is responsible for autosomal recessive arthrogryposis. *Hum. Mol. Genet.*, **18**, 3462–3469.
5. Warren, D.T., Zhang, Q., Weissberg, P.L. and Shanahan, C.M. (2005) Nesprins: intracellular scaffolds that maintain cell architecture and coordinate cell function? *Expert. Rev. Mol. Med.*, **7**, 1–15.
6. Zhang, Q., Skepper, J.N., Yang, F., Davies, J.D., Hegyi, L., Roberts, R.G., Weissberg, P.L., Ellis, J.A. and Shanahan, C.M. (2001) Nesprins: a novel family of spectrin-repeat-containing proteins that localize to the nuclear membrane in multiple tissues. *J. Cell Sci.*, **114**, 4485–4498.
7. Wilhelmsen, K., Litjens, S.H., Kuikman, I., Tshimbalanga, N., Janssen, H., van den Bout, I., Raymond, K. and Sonnenberg, A. (2005) Nesprin-3, a novel outer nuclear membrane protein, associates with the cytoskeletal linker protein plectin. *J. Cell Biol.*, **171**, 799–810.
8. Roux, K.J., Crisp, M.L., Liu, Q., Kim, D., Kozlov, S., Stewart, C.L. and Burke, B. (2009) Nesprin 4 is an outer nuclear membrane protein that can induce kinesin-mediated cell polarization. *Proc. Natl Acad. Sci. USA*, **106**, 2194–2199.
9. Zhang, Q., Ragnauth, C., Skepper, J., Worth, N., Warren, D., Roberts, R., Weissberg, P., Ellis, J. and Shanahan, C. (2005) Nesprin-2 is a multi-isomeric protein that binds lamin and emerin at the nuclear envelope and forms a subcellular network in skeletal muscle. *J. Cell Sci.*, **118**, 673–687.
10. Padmakumar, V.C., Abraham, S., Braune, S., Noegel, A.A., Tunggal, B., Karakesisoglou, I. and Korenbaum, E. (2004) Enaptin, a giant actin-binding protein, is an element of the nuclear membrane and the actin cytoskeleton. *Exp. Cell Res.*, **295**, 330–339.
11. Zhen, Y.Y., Libotte, T., Munck, M., Noegel, A.A. and Korenbaum, E. (2002) NUANCE, a giant protein connecting the nucleus and actin cytoskeleton. *J. Cell Sci.*, **115**, 3207–3222.
12. Crisp, M., Liu, Q., Roux, K., Rattner, J.B., Shanahan, C., Burke, B., Stahl, P.D. and Hodzic, D. (2006) Coupling of the nucleus and cytoplasm: role of the LINC complex. *J. Cell Biol.*, **172**, 41–53.
13. Padmakumar, V.C., Libotte, T., Lu, W., Zaim, H., Abraham, S., Noegel, A.A., Gotzmann, J., Foisner, R. and Karakesisoglou, I. (2005) The inner nuclear membrane protein Sun1 mediates the anchorage of Nesprin-2 to the nuclear envelope. *J. Cell Sci.*, **118**, 3419–3430.
14. Lei, K., Zhang, X., Ding, X., Guo, X., Chen, M., Zhu, B., Xu, T., Zhuang, Y., Xu, R. and Han, M. (2009) SUN1 and SUN2 play critical but partially redundant roles in anchoring nuclei in skeletal muscle cells in mice. *Proc. Natl Acad. Sci. USA*, **106**, 10207–10212.
15. Stewart-Hutchinson, P., Hale, C., Wirtz, D. and Hodzic, D. (2008) Structural requirements for the assembly of LINC complexes and their function in cellular mechanical stiffness. *Exp. Cell Res.*, **314**, 1892–1905.
16. Mislow, J.M., Kim, M.S., Davis, D.B. and McNally, E.M. (2002) Myne-1, a spectrin repeat transmembrane protein of the myocyte inner nuclear membrane, interacts with lamin A/C. *J. Cell Sci.*, **115**, 61–70.

17. Mislow, J.M., Holaska, J.M., Kim, M.S., Lee, K.K., Segura-Totten, M., Wilson, K.L. and McNally, E.M. (2002) Nesprin-1alpha self-associates and binds directly to emerin and lamin A *in vitro*. *FEBS Lett.*, **525**, 135–140.
18. Guild, G.M., Connelly, P.S., Shaw, M.K. and Tilney, L.G. (1997) Actin filament cables in *Drosophila* nurse cells are composed of modules that slide passively past one another during dumping. *J. Cell Biol.*, **138**, 783–797.
19. Ketelaar, T., Faivre-Moskalenko, C., Esseling, J.J., de Ruijter, N.C., Grierson, C.S., Dogterom, M. and Emons, A.M. (2002) Positioning of nuclei in *Arabidopsis* root hairs: an actin-regulated process of tip growth. *Plant Cell*, **14**, 2941–2955.
20. Starr, D.A. and Han, M. (2002) Role of ANC-1 in tethering nuclei to the actin cytoskeleton. *Science*, **298**, 406–409.
21. Yu, J., Starr, D.A., Wu, X., Parkhurst, S.M., Zhuang, Y., Xu, T., Xu, R. and Han, M. (2006) The KASH domain protein MSP-300 plays an essential role in nuclear anchoring during *Drosophila* oogenesis. *Dev. Biol.*, **289**, 336–345.
22. Grady, R.M., Starr, D.A., Ackerman, G.L., Sanes, J.R. and Han, M. (2005) Syne proteins anchor muscle nuclei at the neuromuscular junction. *Proc. Natl Acad. Sci. USA*, **102**, 4359–4364.
23. Luke, Y., Zaim, H., Karakesisoglou, I., Jaeger, V.M., Sellin, L., Lu, W., Schneider, M., Neumann, S., Beijer, A., Munck, M. *et al.* (2008) Nesprin-2 Giant (NUANCE) maintains nuclear envelope architecture and composition in skin. *J. Cell Sci.*, **121**, 1887–1898.
24. Zhang, X., Xu, R., Zhu, B., Yang, X., Ding, X., Duan, S., Xu, T., Zhuang, Y. and Han, M. (2007) Syne-1 and Syne-2 play crucial roles in myonuclear anchorage and motor neuron innervation. *Development*, **134**, 901–908.
25. Puckelwartz, M.J., Kessler, E., Zhang, Y., Hodzic, D., Randles, K.N., Morris, G., Earley, J.U., Hadhazy, M., Holaska, J.M., Mewborn, S.K. *et al.* (2009) Disruption of nesprin-1 produces an Emery Dreifuss muscular dystrophy-like phenotype in mice. *Hum. Mol. Genet.*, **18**, 607–620.
26. Simpson, J.G. and Roberts, R.G. (2008) Patterns of evolutionary conservation in the nesprin genes highlight probable functionally important protein domains and isoforms. *Biochem. Soc. Trans.*, **36**, 1359–1367.
27. Apel, E., Lewis, R., Grady, R. and Sanes, J. (2000) Syne-1, a dystrophin- and Klarsicht-related protein associated with synaptic nuclei at the neuromuscular junction. *J. Biol. Chem.*, **275**, 31986–31995.
28. Zhang, Q., Skepper, J., Yang, F., Davies, J., Hegyi, L., Roberts, R., Weissberg, P., Ellis, J. and Shanahan, C. (2001) Nesprins: a novel family of spectrin-repeat-containing proteins that localize to the nuclear membrane in multiple tissues. *J. Cell Sci.*, **114**, 4485–4498.
29. O'Gorman, S., Dagenais, N.A., Qian, M. and Marchuk, Y. (1997) Protamine-Cre recombinase transgenes efficiently recombine target sequences in the male germ line of mice, but not in embryonic stem cells. *Proc. Natl Acad. Sci. USA*, **94**, 14602–14607.
30. Lammerding, J., Hsiao, J., Schulze, P.C., Kozlov, S., Stewart, C.L. and Lee, R.T. (2005) Abnormal nuclear shape and impaired mechanotransduction in emerin-deficient cells. *J. Cell Biol.*, **170**, 781–791.
31. Sam, M., Shah, S., Friden, J., Milner, D.J., Capetanaki, Y. and Lieber, R.L. (2000) Desmin knockout muscles generate lower stress and are less vulnerable to injury compared with wild-type muscles. *Am. J. Physiol. Cell. Physiol*, **279**, C1116–C1122.
32. Gokhin, D.S., Bang, M.L., Zhang, J., Chen, J. and Lieber, R.L. (2009) Reduced thin filament length in nebulin-knockout skeletal muscle alters isometric contractile properties. *Am. J. Physiol. Cell. Physiol*, **296**, C1123–C1132.
33. Lee, J.S., Hale, C.M., Panorchan, P., Khatau, S.B., George, J.P., Stewart, C.L., Hodzic, D. and Wirtz, D. (2007) Effects of nuclear lamin A/C deficiency on cell mechanics, polarization and migration. *Biophys. J.*, **93**, 2542–2552.
34. Shah, S.B., Davis, J., Weisleder, N., Kostavassili, I., McCulloch, A.D., Ralston, E., Capetanaki, Y. and Lieber, R.L. (2004) Structural and functional roles of desmin in mouse skeletal muscle during passive deformation. *Biophys. J.*, **86**, 2993–3008.
35. Houben, F., Ramaekers, F.C., Snoeckx, L.H. and Broers, J.L. (2007) Role of nuclear lamina-cytoskeleton interactions in the maintenance of cellular strength. *Biochim. Biophys. Acta*, **1773**, 675–686.
36. Ingber, D.E. (2003) Tensegrity II. How structural networks influence cellular information processing networks. *J. Cell Sci.*, **116**, 1397–1408.
37. Ingber, D.E. (2006) Cellular mechanotransduction: putting all the pieces together again. *FASEB J.*, **20**, 811–827.
38. Lammerding, J., Fong, L.G., Ji, J.Y., Reue, K., Stewart, C.L., Young, S.G. and Lee, R.T. (2006) Lamins A and C but not lamin B1 regulate nuclear mechanics. *J. Biol. Chem.*, **281**, 25768–25780.
39. Sullivan, T., Escalante-Alcalde, D., Bhatt, H., Anver, M., Bhat, N., Nagashima, K., Stewart, C.L. and Burke, B. (1999) Loss of A-type lamin expression compromises nuclear envelope integrity leading to muscular dystrophy. *J. Cell Biol.*, **147**, 913–920.
40. Melcon, G., Kozlov, S., Cutler, D.A., Sullivan, T., Hernandez, L., Zhao, P., Mitchell, S., Nader, G., Bakay, M., Rottman, J.N. *et al.* (2006) Loss of emerin at the nuclear envelope disrupts the Rb1/E2F and MyoD pathways during muscle regeneration. *Hum. Mol. Genet.*, **15**, 637–651.
41. Frock, R.L., Kudlow, B.A., Evans, A.M., Jameson, S.A., Hauschka, S.D. and Kennedy, B.K. (2006) Lamin A/C and emerin are critical for skeletal muscle satellite cell differentiation. *Genes Dev.*, **20**, 486–500.
42. Chen, J., Kubalak, S.W., Minamisawa, S., Price, R.L., Becker, K.D., Hickey, R., Ross, J. Jr and Chien, K.R. (1998) Selective requirement of myosin light chain 2v in embryonic heart function. *J. Biol. Chem.*, **273**, 1252–1256.
43. Bang, M., Li, X., Littlefield, R., Bremner, S., Thor, A., Knowlton, K., Lieber, R. and Chen, J. (2006) Nebulin-deficient mice exhibit shorter thin filament lengths and reduced contractile function in skeletal muscle. *J. Cell Biol.*, **173**, 905–916.
44. Dubowitz, V., Sewry, C.A. and Lane, R.J.M. (2007) *Muscle Biopsy: a Practical Approach*, Saunders Elsevier, Philadelphia.
45. Burkholder, T.J., Fingado, B., Baron, S. and Lieber, R.L. (1994) Relationship between muscle fiber types and sizes and muscle architectural properties in the mouse hindlimb. *J. Morphol.*, **221**, 177–190.
46. Mendez, J. and Keys, A. (1960) Density and composition of mammalian muscle. *Metabolism-Clinical and Experimental*, **9**, 184–188.
47. Shah, S.B. and Lieber, R.L. (2003) Simultaneous imaging and functional assessment of cytoskeletal protein connections in passively loaded single muscle cells. *J. Histochem. Cytochem.*, **51**, 19–29.